Odderon Physics at High Energies

Emerson Luna

Instituto de Física

Universidade Federal do Rio Grande do Sul

XVI International Workshop on Hadron Physics

Porto Alegre, 2025

Outline

- Brief introduction to Odderon
- Formalism: Pomeron and Odderon inputs
- The tension between the TOTEM and ALFA/ATLAS measurements
- Results
- Conclusions

Introduction

■ The TOTEM publication of the measurements of the σ_{tot}^{pp} and the ρ^{pp} parameter at 13 TeV, prompted a renewal of interest in the potential existence of the high-energy C-odd (Odderon) contribution.

$\Rightarrow$ The observed value $\rho = (0.09 - 0.10) \pm 0.01$ turned out to be smaller than the predicted value ($\rho = 0.13 - 0.14$) based on Disp. Rel.

□ The new ATLAS/ALFA data recently confirmed this value of ρ

$\Rightarrow$ However, the value of σ_{tot}^{pp} at 13 TeV reported by the ATLAS/ALFA team is approximately 5% lower than the average of values determined by TOTEM

Introduction

■ The relatively small value of ρ can be explained by the admixture of the *C*-odd amplitude, which survives at high LHC energies

■ Theoretically there are reasons to have *no* such an amplitude

$\Rightarrow$ Such amplitude with the intercept α_{Odd} close to 1 was predicted by the perturbative QCD

□ Another indication in favor of the Odderon emerged when the $d\sigma^{\bar{p}p}/dt$ data at $\sqrt{s} = 1.96$ TeV was compared with the corresponding pp cross section (measured at 2.76 TeV but extrapolated to 1.96 TeV) in the diffractive dip region

$\Rightarrow$ A clear difference was observed

Introduction

■ It should be noted that at very low t close to zero and in the diffractive dip region, we deal with different C-odd contributions

$\Rightarrow$ To get a well-pronounced dip-bump structure near the dip in $d\sigma^{pp}/dt|_{2.76\,TeV}$ and rather flat behavior of $d\sigma^{\bar{p}p}/dt\big|_{1.96\,TeV}$, the real part of the Odderon pp amplitude should be positive (in agreement with perturbative QCD expectation for the three gluon exchange)

$\Rightarrow$ On the other hand, to explain the low value of ρ at $t = 0$, we need a negative Odderon real part

$\Rightarrow$ This negative real part could be induced by non-pert. effects

Formalism

■ Our analysis is focused on differential cross-section data involving very small values of t

$\Rightarrow$ It requires consideration of the Coulomb-nuclear interference (CNI) region:

$$F^{C+N} = F^N + e^{i\alpha\phi(t)} F^C$$

□ We adopt

$$\phi(t) = \kappa \left[\gamma + \ln\left(\frac{B|t|}{2}\right) + \ln\left(1 + \frac{8}{B\Lambda^2}\right) + \frac{4|t|}{\Lambda^2} \ln\left(\frac{\Lambda^2}{4|t|}\right) - \frac{2|t|}{\Lambda^2} \right]$$

where κ flips sign when going from pp ($\kappa = -1$) to $\bar{p}p$ ($\kappa = +1$)

Formalism

$\Rightarrow \Lambda^2$ is fixed at $0.71\ \mathrm{GeV}^2$

$\Rightarrow B$ is the t slope of elastic $d\sigma/dt \propto exp(Bt)$ cross-section

$\Rightarrow \gamma = 0.577...$ is the Euler-Mascheroni constant

$\Rightarrow \alpha$ is the electromagnetic coupling:

$$\alpha(q^2) = \frac{\alpha(0)}{1 - \frac{\alpha(0)}{3\pi} \ln\left(\frac{q^2+m_e^2}{m_e^2}\right)}$$

where $\alpha(0) \approx 1/137$

- The Coulomb amplitude is expressed as

$$F^C = \kappa s \frac{2\alpha}{|t|} G^2(t)$$

where $G(t)$ is the electromagnetic form factor of the proton:

$$G(t) = \left[\frac{\Lambda^2}{\Lambda^2 + q^2}\right]^2$$

- To account for the eikonalization [1]:

$$\Omega_i(s,b) = \frac{2}{s}\int_0^\infty q\, dq\, J_0(bq)\, F_i^N(s,t)$$

where $i = \mathbb{P}, \mathbb{O}$ represent the Pomeron and Odderon exchanges

[1] E.G.S. Luna, M.G. Ryskin, Phys. Rev. D **110** (2024) 094007

Pomeron input

- The single Pomeron contribution is given by

$$F_{\mathbb{P}}^{N}(s,t) = \beta_{\mathbb{P}}^{2}(t)\,\eta_{\mathbb{P}}(t)\left(\frac{s}{s_0}\right)^{\alpha_{\mathbb{P}}(t)}$$

$\Rightarrow \eta_{\mathbb{P}}(t) = -e^{-i\frac{\pi}{2}\alpha_{\mathbb{P}}(t)}$ is the even signature factor

$\Rightarrow \beta_{\mathbb{P}}(t)$ is the elastic proton-Pomeron vertex

$\Rightarrow \alpha_{\mathbb{P}}(t)$ is the Pomeron trajectory,

$$\alpha_{\mathbb{P}}(t) = 1 + \epsilon + \alpha'_{\mathbb{P}} t + \frac{m_\pi^2 \beta_\pi^2}{32\pi^3}\, h(\tau)$$

where

$$h(\tau) = -\frac{4}{\tau}\, F_\pi^2(t)\left[2\tau - (1+\tau)^{3/2}\ln\left(\frac{\sqrt{1+\tau}+1}{\sqrt{1+\tau}-1}\right) + \ln\left(\frac{m^2}{m_\pi^2}\right)\right]$$

with $\epsilon > 0$, $\tau = 4m_\pi^2/|t|$, $m = 1$ GeV, and $m_\pi = 139.6$ MeV

The Odderon input

■ From the standpoint of QCD (at the lowest order) the $C = +1$ amplitude arises from the exchange of two gluons and the $C = -1$ amplitude from the exchange of three gluons

■ Extensive theoretical studies have been directed towards uncovering corrections to these results, particularly in higher orders

□ In this scenario, the leading-log approximation allows for the summation of certain higher-order contributions to physical observables in high-energy particle scattering processes

$\Rightarrow$ This approach was widely used in the study of the QCD-Pomeron through the BFKL equation

The Odderon input

$\Rightarrow$ In BFKL equation terms of the order $(\alpha_s \ln(s))^n$ are systematically summed at high energy (large s) and small strong coupling α_s

$\Rightarrow$ The simplistic notion of bare two-gluon exchange gives way to the BFKL Pomeron, which, in an alternative representation, can be seen as the interaction of two reggeized gluons with one another

■ Beyond the BFKL Pomeron, the most elementary entity within perturbative QCD is the exchange involving three interacting reggeized gluons

□ The evolution of the three-gluon Odderon exchange as energy increases is governed by the BKP equation

$\Rightarrow$ A bound state solution of this Odderon equation was obtained with the intercept $\alpha_{\mathbb{O}}(0) = 1$

The Odderon input

- Based on these QCD findings, we adopt in this work the simplest conceivable form for the Odderon trajectory:

$$\alpha_{\mathbb{O}}(t) = 1$$

- The Odderon contribution is given by

$$F_{\mathbb{O}}^{N}(s,t) = \beta_{\mathbb{O}}^{2}(t)\,\eta_{\mathbb{O}}(t)\left(\frac{s}{s_0}\right)^{\alpha_{\mathbb{O}}(t)}$$

$\Rightarrow \eta_{\mathbb{O}}(t) = -ie^{-i\frac{\pi}{2}\alpha_{\mathbb{O}}(t)}$ is the odd signature factor

$\Rightarrow \beta_{\mathbb{O}}(t)$ is the elastic proton-Odderon vertex

t dependence of the β vertices

■ $\beta_{\mathbb{P}}(t)$ and $\beta_{\mathbb{O}}(t)$ are parameterized accounting for the observed deviation from a pure exponential behavior of the low-$|t|$ $d\sigma/dt$ data at LHC energies

$\Rightarrow$ Behavior identified by the TOTEM Collaboration

□ The TOTEM group has extended the pure exponential to a cumulant expansion,

$$\frac{d\sigma}{dt}(t) = \left.\frac{d\sigma}{dt}\right|_{t=0} \exp\left(\sum_{n=1}^{N_b} b_n t^n\right)$$

where the optimal fit was achieved for $N_b = 3$, yielding $\chi^2/DoF = 1.22$ and a corresponding p-value of 8.0%

t dependence of the β vertices

- Based on this result, we have written the Pomeron- and Odderon-proton vertices as

$$\beta_{\mathbb{P}}(t) = \beta_{\mathbb{P}}(0) e^{\left(At + Bt^2 + Ct^3\right)/2}$$

and

$$\beta_{\mathbb{O}}(t) = \beta_{\mathbb{O}}(0) e^{Dt/2}$$

respectively

Models

■ We allow for the low mass diffractive dissociation (Good-Walker formalism)

$\Rightarrow$ The Pomeron and Odderon couplings to the two diffractive states $|\phi_k\rangle$ are

$$\beta_{i,k}(t) = (1 \pm \gamma)\beta_i(t)$$

with $i = \mathbb{P}$ or $\mathbb{O}$, and $\gamma = 0.55$

□ The eikonalized amplitude in (s,t)-space is then given by

$$\begin{aligned}\mathcal{A}(s,t) \;=\; & is \int_0^\infty b\, db\, J_0(bq) \left[1 - \frac{1}{4}\, e^{i(1+\gamma)^2\Omega(s,b)/2}\right. \\ & \left. -\frac{1}{2}\, e^{i(1-\gamma^2)\Omega(s,b)/2} - \frac{1}{4}\, e^{i(1-\gamma)^2\Omega(s,b)/2}\right]\end{aligned}$$

where $\Omega(s,b)$ is the total opacity

Models

■ We consider two versions for the total opacity with different signs for the Odderon contribution

□ In the first version, referred to as 'Model **I**', we have

$$\Omega(s,b) = \Omega_{\mathbb{P}}(s,b) \mp \Omega_{\mathbb{O}}(s,b)$$

□ In the second version, called 'Model **II**', we have

$$\Omega(s,b) = \Omega_{\mathbb{P}}(s,b) \pm \Omega_{\mathbb{O}}(s,b)$$

$\Rightarrow$ In both cases the upper sign is for pp and the lower sign is for $\bar{p}p$

Models

- The total cross section and the ρ parameter are expressed in terms of the nuclear eikonalized amplitude $\mathcal{A}(s,t)$:

$$\sigma_{tot}(s) = \frac{4\pi}{s}\,\mathrm{Im}\,\mathcal{A}(s,t=0)$$

$$\rho(s) = \frac{\mathrm{Re}\,\mathcal{A}(s,t=0)}{\mathrm{Im}\,\mathcal{A}(s,t=0)}$$

- The full scattering amplitude is written as

$$F^{C+N}(s,t) = \mathcal{A}(s,t) + e^{i\alpha\phi(t)}F^{C}(s,t)$$

- Finally, the differential and the total elastic cross sections are given by

$$\frac{d\sigma}{dt}(s,t) = \frac{\pi}{s^2}\left|\mathcal{A}(s,t) + e^{i\alpha\phi}\mathcal{F}^C(s,t)\right|^2$$

and

$$\sigma_{el}(s) = \frac{\pi}{s^2}\int_{-\infty}^{0} dt\,|\mathcal{A}(s,t)|^2$$

Tension TOTEM versus ATLAS

■ The LHC has released exceptionally precise measurements of diffractive processes

□ These measurements, particularly the total and differential cross sections obtained from ATLAS and TOTEM Collaborations, enable us to determine the Pomeron and Odderon parameters accurately

$\Rightarrow$ However, these experimental results unveil a noteworthy tension between the TOTEM and ATLAS measurements

$\Rightarrow$ For instance, when comparing the TOTEM and the ATLAS result for σ_{tot}^{pp} at $\sqrt{s} = 8$ TeV, the discrepancy between the values corresponds to 2.6 σ

Tension TOTEM versus ATLAS [2]

■ We perform global fits to pp and $\bar{p}p$ differential cross-section data while considering three distinct datasets:

Ensemble A: $\left.\frac{d\sigma^{\bar{p}p,pp}}{dt}\right|_{\text{CERN-ISR}} + \left.\frac{d\sigma^{\bar{p}p}}{dt}\right|_{S\bar{p}pS} + \left.\frac{d\sigma^{\bar{p}p}}{dt}\right|_{\text{Tevatron}} + \left.\frac{d\sigma^{pp}}{dt}\right|_{\text{ATLAS/ALFA}}$

Ensemble T: $\left.\frac{d\sigma^{\bar{p}p,pp}}{dt}\right|_{\text{CERN-ISR}} + \left.\frac{d\sigma^{\bar{p}p}}{dt}\right|_{S\bar{p}pS} + \left.\frac{d\sigma^{\bar{p}p}}{dt}\right|_{\text{Tevatron}} + \left.\frac{d\sigma^{pp}}{dt}\right|_{\text{TOTEM}}$

Ensemble A$\oplus$T: $\left.\frac{d\sigma^{\bar{p}p,pp}}{dt}\right|_{\text{CERN-ISR}} + \left.\frac{d\sigma^{\bar{p}p}}{dt}\right|_{S\bar{p}pS} + \left.\frac{d\sigma^{\bar{p}p}}{dt}\right|_{\text{Tevatron}} + \left.\frac{d\sigma^{pp}}{dt}\right|_{\text{ATLAS/ALFA}} + \left.\frac{d\sigma^{pp}}{dt}\right|_{\text{TOTEM}}$

$\Rightarrow$ We carry out global fits to the two distinct ensembles using a χ^2 fitting procedure, where χ^2_{min} follows a χ^2 distribution with ν DoF

$\Rightarrow$ We adopt an interval $\chi^2 - \chi^2_{min}$ corresponding to a 90% CL.

---

[2] E.G.S. Luna, V.A. Khoze, M.G. Ryskin, Phys. Rev. D **110** (2024) 014002

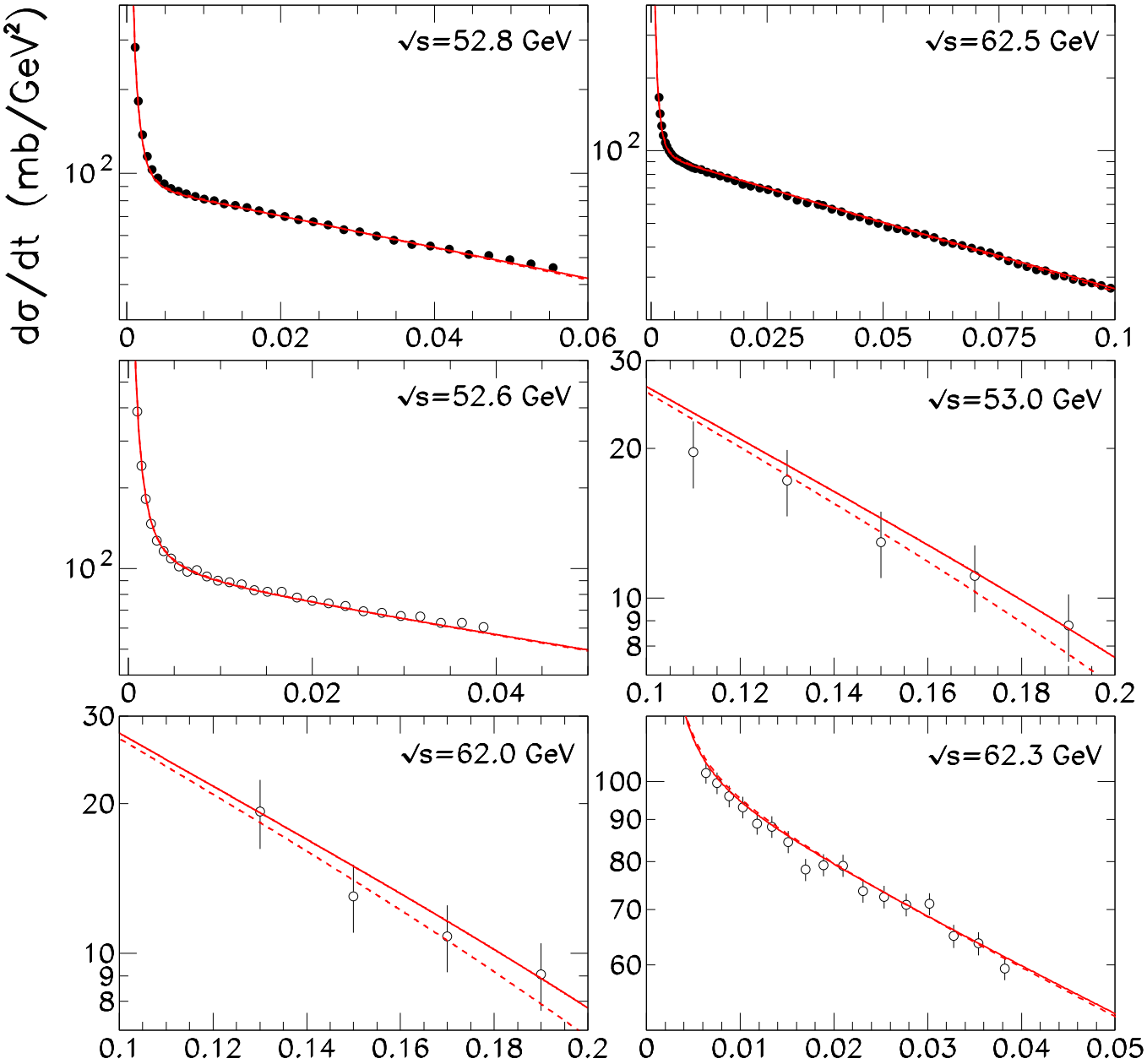

FIG.1. Description of the t dependence of the elastic pp- and $\bar{p}p$-cross sections measured at CERN-ISR. The dashed and solid curves depict the results obtained using Models I and II, respectively

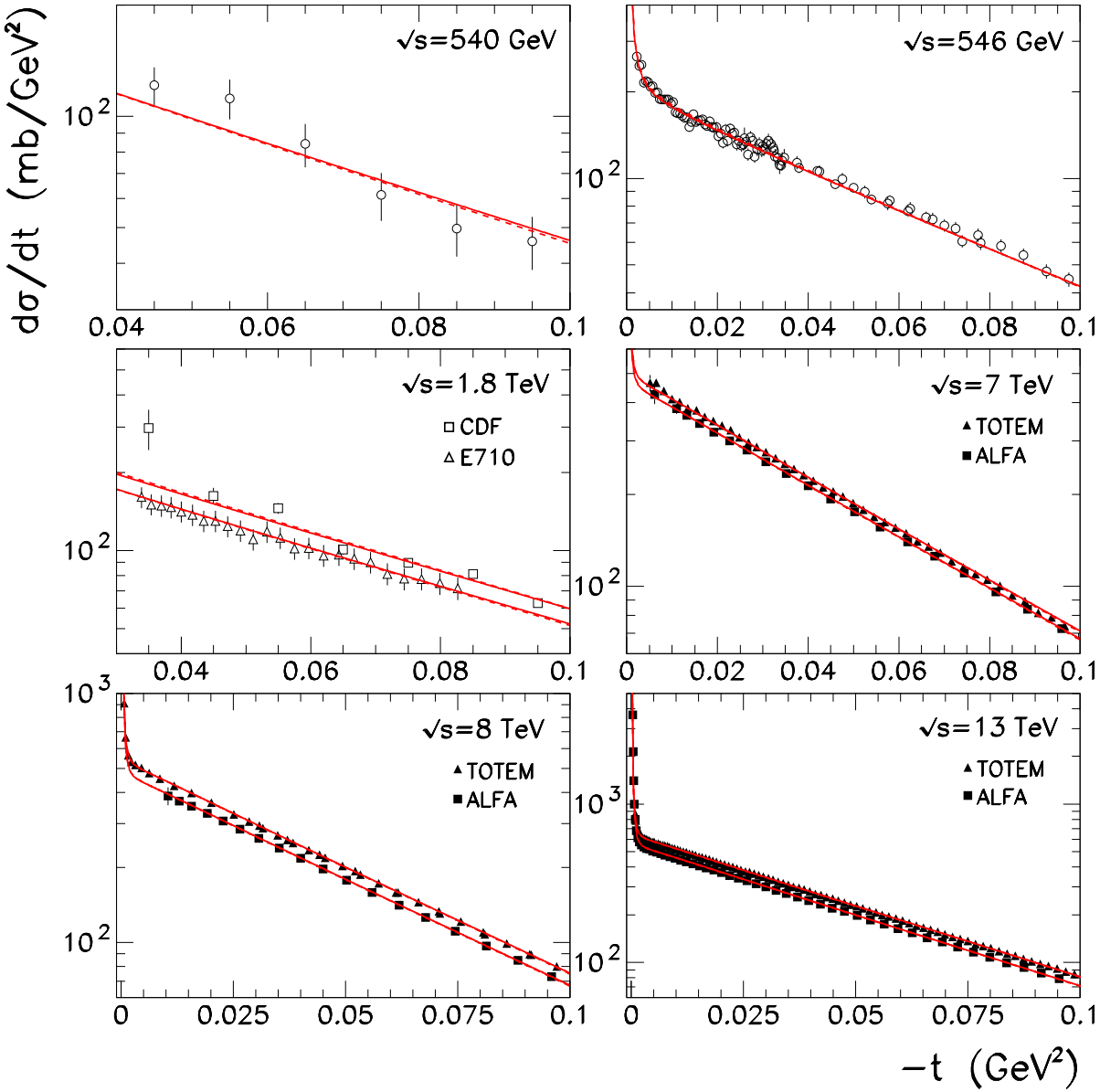

FIG.2. Description of the t dependence of the elastic pp- and $\bar{p}p$-cross sections measured at the $S\bar{p}pS$, the Tevatron and the LHC colliders. The dashed and solid curves depict the results obtained using Models I and II, respectively. The lower curves describe the ATLAS/ALFA (E710) data while the upper curves correspond to the TOTEM (CDF) data; in both cases, the normalization factors N_i are accounted for

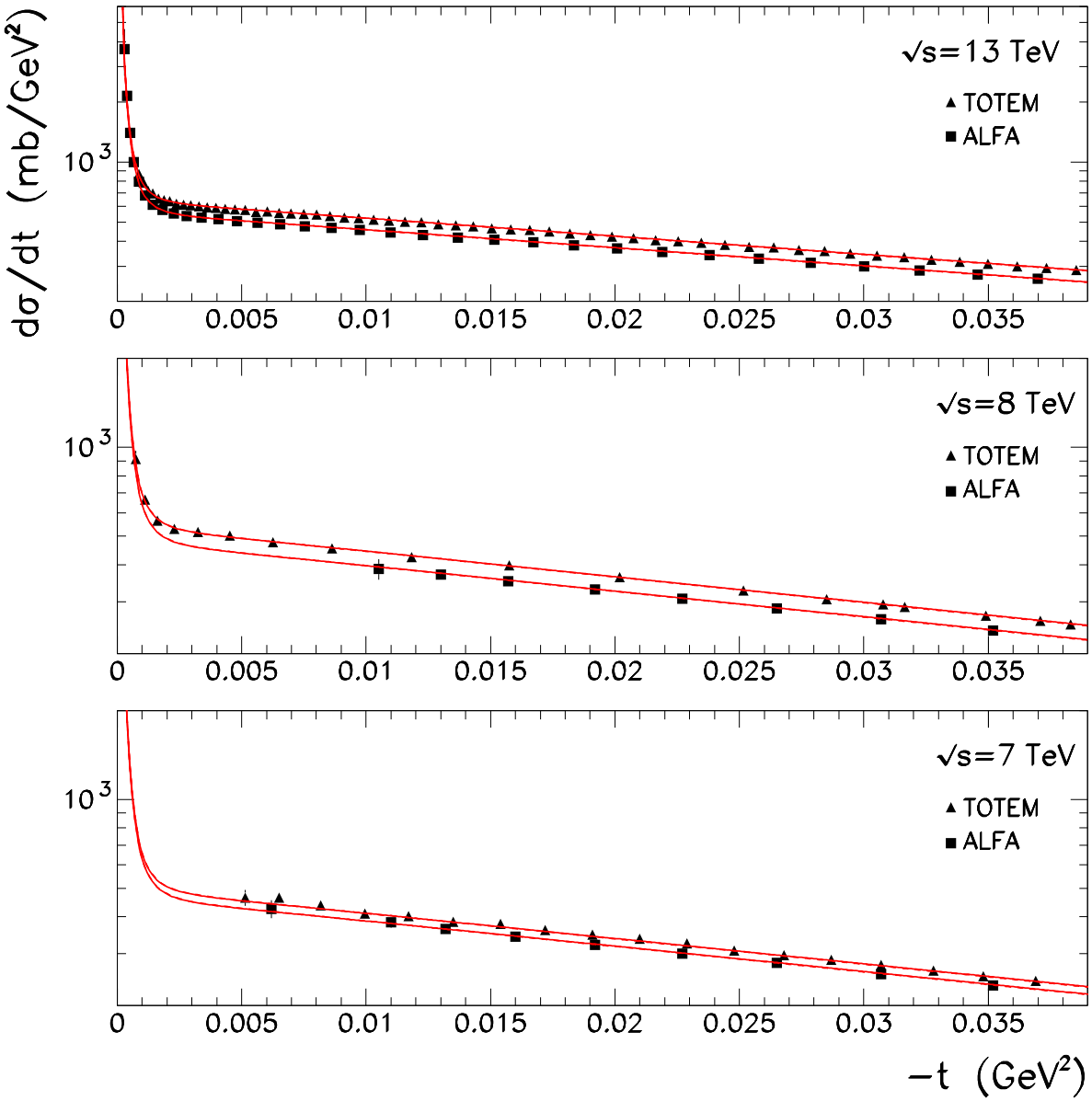

FIG.3. The same as Fig. 2 but for the CNI region where the Odderon contribution reveals itself

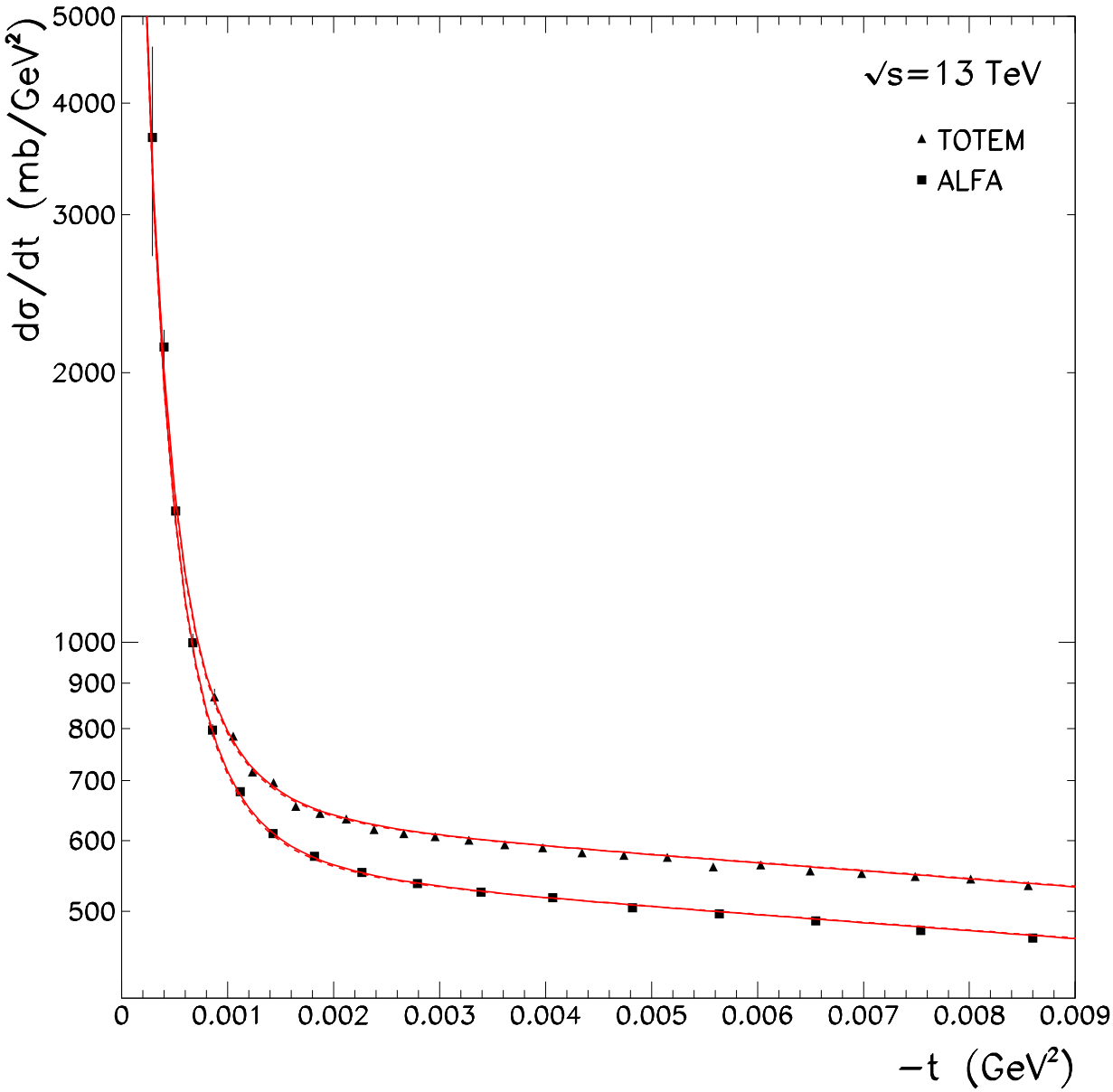

FIG.4. The same as Figs. 2 and 3 but in another scale to better see the quality of precise 13 TeV data description

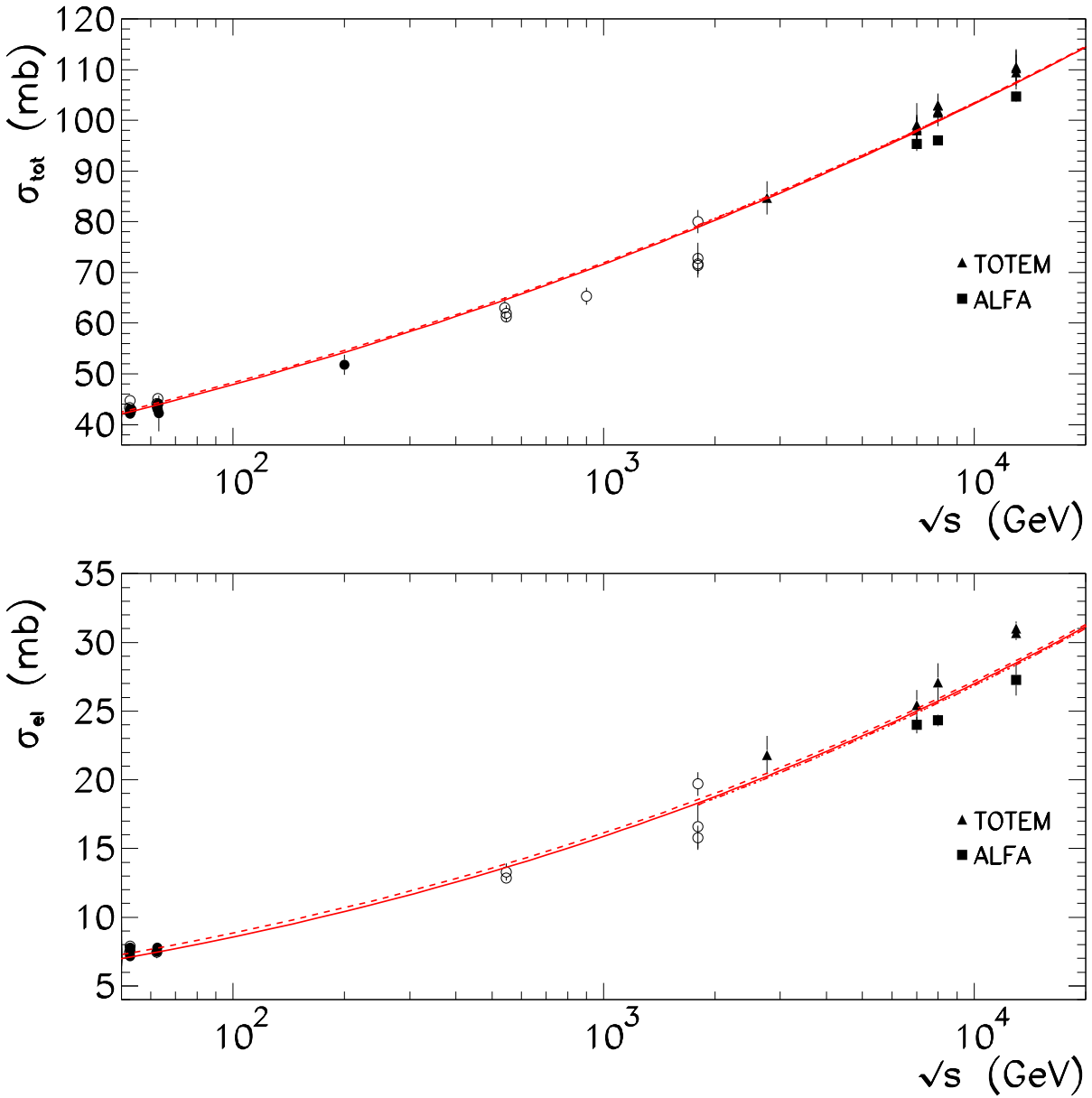

FIG.5. Description of the total and elastic pp (●, ▲, ■) and $\bar{p}p$ (○) cross sections. The dotted and dashed-dotted curves represent the results for pp and $\bar{p}p$ channels, respectively, obtained from the global fit to Ensemble A $\oplus$ T using Model I. These curves are indistinguishable. The solid and dashed curves represent the results for pp and $\bar{p}p$ channels, respectively, obtained from the global fit to Ensemble A $\oplus$ T using Model II

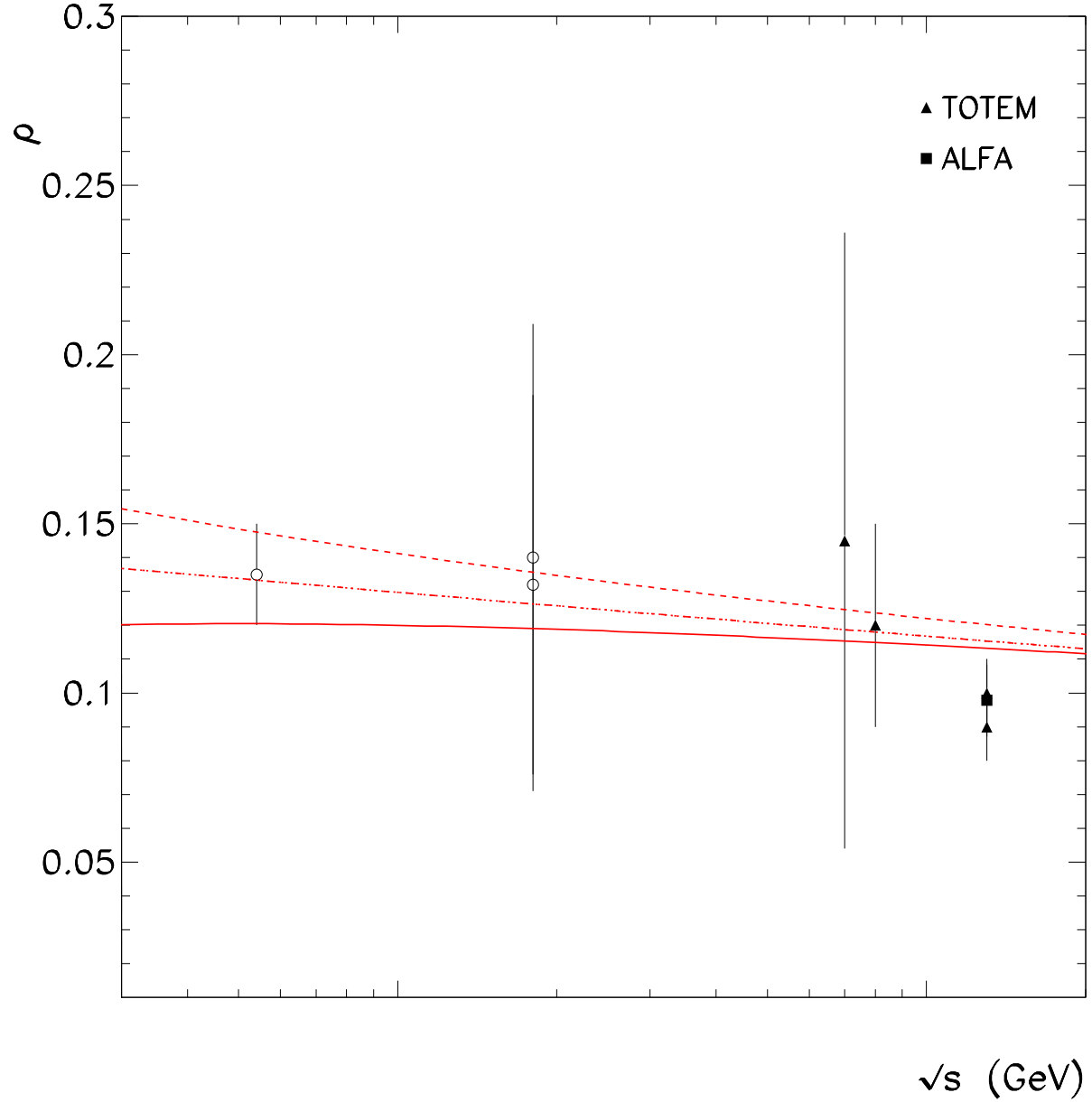

FIG.6. ρ parameter for pp (▲, ■) and $\bar{p}p$ (○) elastic amplitude. The dotted and dashed-dotted curves represent the results for ρ^{pp} and $\rho^{\bar{p}p}$, respectively, obtained from the global fit to Ensemble A $\oplus$ T using the Model I. These curves are indistinguishable. The solid and dashed curves represent the results for ρ^{pp} and $\rho^{\bar{p}p}$, respectively, obtained from the global fit to Ensemble A $\oplus$ T using the Model II

Table: Predictions for $\sigma_{tot}^{\bar{p}p,pp}$, $\sigma_{el}^{\bar{p}p,pp}$, and $\rho^{\bar{p}p,pp}$ using Models I and II. These results were derived for the scenario with $D = A/2$

	Model I			Model II		
$\sqrt{s}$ (TeV)	$\sigma_{tot}^{pp} \mid \sigma_{tot}^{\bar{p}p}$ (mb)	$\sigma_{el}^{pp} \mid \sigma_{el}^{\bar{p}p}$ (mb)	$\rho^{pp} \mid \rho^{\bar{p}p}$	$\sigma_{tot}^{pp} \mid \sigma_{tot}^{\bar{p}p}$ (mb)	$\sigma_{el}^{pp} \mid \sigma_{el}^{\bar{p}p}$ (mb)	$\rho^{pp} \mid \rho^{\bar{p}p}$
0.541	64.2 | 64.2	13.2 | 13.2	0.130 | 0.130	63.8 | 64.1	13.3 | 13.5	0.117 | 0.144
1.8	78.0 | 78.0	17.6 | 17.6	0.124 | 0.124	77.6 | 77.8	17.7 | 17.9	0.116 | 0.133
7	95.9 | 95.9	23.9 | 23.9	0.117 | 0.117	95.7 | 95.9	24.0 | 24.2	0.113 | 0.123
8	97.9 | 97.9	24.5 | 24.5	0.116 | 0.116	97.6 | 97.8	24.7 | 24.8	0.113 | 0.122
13	105.1 | 105.1	27.2 | 27.2	0.114 | 0.114	104.9 | 105.1	27.3 | 27.4	0.111 | 0.119

Table: Results using Model II

			Ensemble A		
D (GeV^{-2})	$0.1A$	$0.3A$	$0.5A$	$0.7A$	$0.9A$
$\beta_{\mathbb{O}}(0)$	0.93±0.22	0.85±0.22	0.80±0.21	0.77±0.19	0.74±0.18
$\beta_{\mathbb{P}}(0)$	2.370±0.035	2.384±0.036	2.386±0.037	2.386±0.040	2.388±0.039
ν	332	332	332	332	332
χ^2/ν	0.96	0.97	0.97	0.97	0.96
$\rho^{pp}(\sqrt{s} = 13$ TeV)	0.105	0.105	0.105	0.104	0.104
$\rho^{\bar{p}p}(\sqrt{s} = 13$ TeV)	0.113	0.112	0.113	0.114	0.114
$\sigma_{tot}^{pp}(\sqrt{s} = 13$ TeV) (mb)	98.0	98.0	98.0	98.0	98.0
$\sigma_{tot}^{pp}(\sqrt{s} = 13$ TeV) (mb)	98.2	98.2	98.2	98.2	98.1
			Ensemble T		
D (GeV^{-2})	$0.1A$	$0.3A$	$0.5A$	$0.7A$	$0.9A$
$\beta_{\mathbb{O}}(0)$	1.09±0.22	0.96±0.18	0.90±0.16	0.86±0.15	0.83±0.14
$\beta_{\mathbb{P}}(0)$	2.236±0.022	2.258±0.016	2.260±0.016	2.260±0.017	2.259±0.018
ν	418	418	418	418	418
χ^2/ν	1.28	1.30	1.29	1.28	1.27
$\rho^{pp}(\sqrt{s} = 13$ TeV)	0.112	0.112	0.111	0.111	0.110
$\rho^{\bar{p}p}(\sqrt{s} = 13$ TeV)	0.119	0.118	0.119	0.119	0.120
$\sigma_{tot}^{pp}(\sqrt{s} = 13$ TeV) (mb)	104.9	104.9	104.9	104.9	104.9
$\sigma_{tot}^{pp}(\sqrt{s} = 13$ TeV) (mb)	105.1	105.1	105.1	105.1	105.1
			Ensemble $A \oplus T$		
D (GeV^{-2})	$0.1A$	$0.3A$	$0.5A$	$0.7A$	$0.9A$
$\beta_{\mathbb{O}}(0)$	1.09±0.24	0.95±0.19	0.90±0.18	0.86±0.17	0.83±0.16
$\beta_{\mathbb{P}}(0)$	2.235±0.023	2.257±0.016	2.259±0.016	2.258±0.016	2.258±0.017
ν	504	504	504	504	504
χ^2/ν	1.11	1.12	1.11	1.10	1.09
$\rho^{pp}(\sqrt{s} = 13$ TeV)	0.112	0.112	0.111	0.111	0.110
$\rho^{\bar{p}p}(\sqrt{s} = 13$ TeV)	0.119	0.118	0.119	0.119	0.120
$\sigma_{tot}^{pp}(\sqrt{s} = 13$ TeV) (mb)	104.9	104.9	104.9	104.9	104.9
$\sigma_{tot}^{pp}(\sqrt{s} = 13$ TeV) (mb)	105.1	105.1	105.1	105.1	105.1

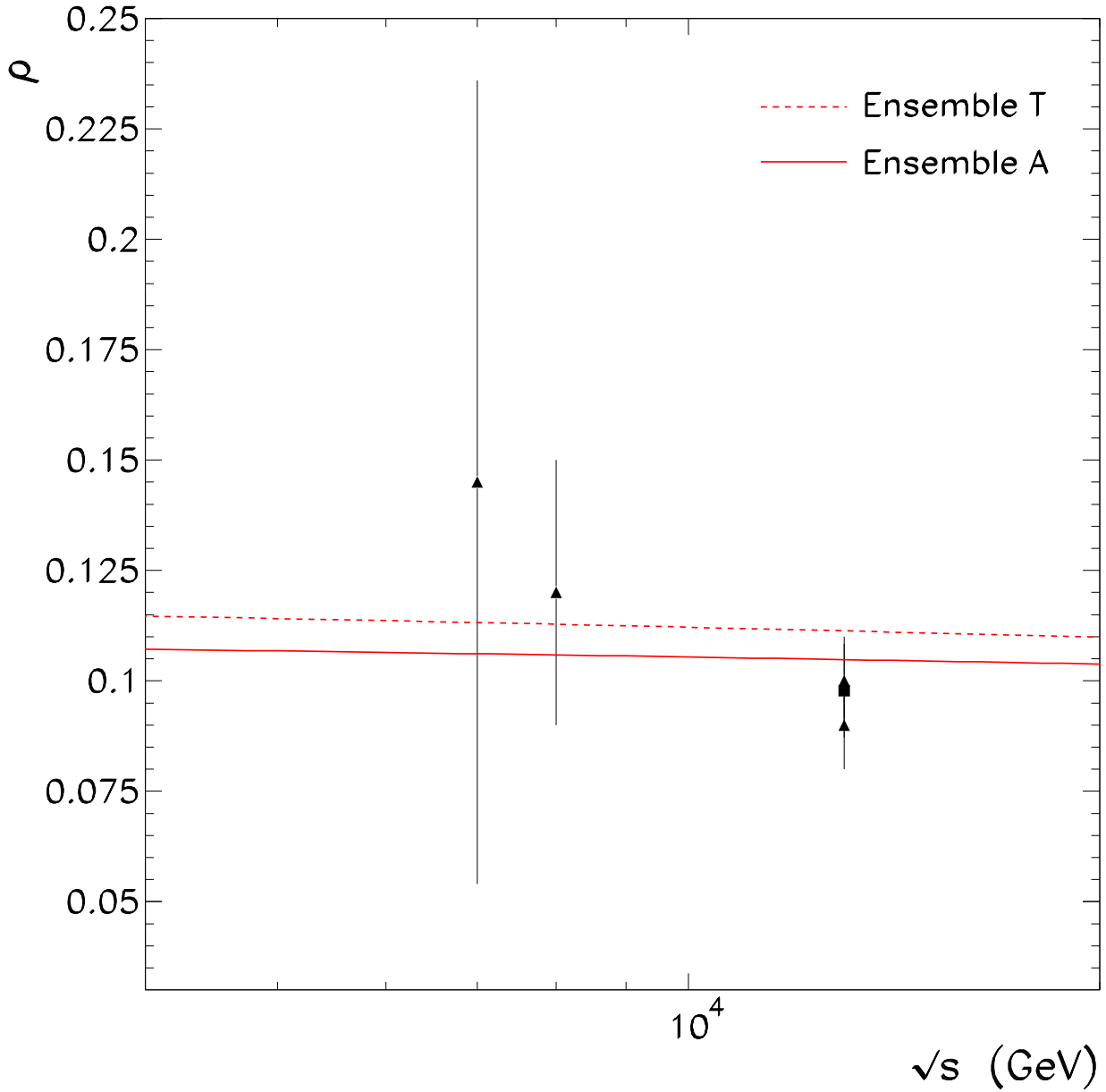

FIG.7. Description of ρ parameter for pp elastic amplitude measured by TOTEM (▲) and ATLAS/ALFA (■) Collaborations. The dashed (solid) curve represents the predicted ρ^{pp} from the global fit using Ensemble T (Ensemble A)

Conclusions

■ The differential pp and $\bar{p}p$ cross sections $d\sigma/dt$ at low $|t| < 0.1$ GeV^2 and collider energies (from $\sqrt{s} > 50$ GeV to 13 TeV) are successfully described ($\chi^2/\nu = 1.11$) within the two-channel eikonal model

□ To avoid the double counting we do not include in the fit the σ_{tot} and ρ data (which were obtained from the description of the same $d\sigma/dt$ data points)

■ The model accounts for the screening of the Odderon contribution by the Pomerons including the C-even (Pomeron) and C-odd (Odderon) multiple exchanges

■ To resolve the discrepancy between the TOTEM and ATLAS/ALFA (CDF and E710 in the Tevatron case) data we introduce the normalization coefficients, N_i writing the theoretical prediction as $d\sigma^{exp}/dt = N_i d\sigma^{Th}/dt$

Conclusions

- We show that the presence of C-odd (Odderon) contribution essentially improves the fit; however it does not noticeably change the predicted value of ρ^{pp} at 13 TeV

- The main lessons about the Odderon coming from this study are:

$\Longrightarrow$ The description using the Odderon improves the fit (the χ^2/ν is the lowest one)

$\Longrightarrow$ The sign of the Odderon amplitude needed to describe the very low $|t|$ data is opposite to that predicted by the perturbative QCD three-gluon exchange contribution

Conclusions

$\Longrightarrow$ The quality of the description weakly depends on the Odderon t-slope, D, (leading to practically the same values of σ_{tot} and ρ).

$\Longrightarrow$ The Odderon-proton coupling, $\beta_{\mathbb{O}}$, is smaller than that for the Pomeron, $\beta_{\mathbb{P}}$. For $D = A/2$ we get $\beta_{\mathbb{O}}/\beta_{\mathbb{P}} = 0.40$

■ The possibility to searching for the Odderon in Ultraperipheral Proton-Ion Collisions at the LHC was discussed in [3]

[3] L.A. Harland-Lang, V.A. Khoze, A.D. Martin, M.G. Ryskin, Phys. Rev. D **110** (2019) 034011

THANK YOU

Resummations in QCD

- Every physical observable can be written, in pQCD, as a power series in α_s

$\Longrightarrow$ in these series the coupling constant is accompanied by large logarithms, which need to be resummed

$\Longrightarrow$ according to the type and to the powers of logarithms that are effectively resummed one gets different evolution equations

- The solution of the DGLAP equation sums over all orders in α_s the contributions from leading, single, collinear logarithms of the form $\alpha_s \ln\left(Q^2/Q_0^2\right)$

$\Longrightarrow$ it does not include leading, single, soft singularities of the form $\alpha_s \ln\left(1/x\right)$, which are treated instead by the BFKL equation

- The BFKL equation describes the x-evolution of PDFs at fixed Q^2

Resummations in QCD

- The phase space regions which contribute these logarithms enhancements are associated with configurations in which successive partons have strongly ordered transverse, k_T, or longitudinal, $k_L \equiv x$, momenta:

  $\Rightarrow \alpha_s L_Q \sim 1$, $\alpha_s L_x \ll 1$: $Q^2 \gg k^2_{T,n} \gg \cdots \gg k^2_{T,1} \gg Q^2_0$

  $\Rightarrow \alpha_s L_x \sim 1$, $\alpha_s L_Q \ll 1$: $x \ll x_n \ll \cdots \ll x_1 \ll x_0$

- At small-x and slow Q^2 (where gluons are dominant) we do not have strongly ordered k_T

  $\Rightarrow$ we have to integrate over the full range of k_T

  $\Rightarrow$ this leads us to work with the *unintegrated* gluon PDF $\tilde{g}(x, k^2_T)$:

$$xg(x, Q^2) = \int^{Q^2} \frac{dk^2_T}{k^2_T} \tilde{g}(x, k^2_T)$$

Positivity

- The phase factor is associated with the positivity property

$\Rightarrow$ However, unlike Pomeron, the Odderon is not constrained by positivity requirements

$\Rightarrow$ From a theoretical standpoint, this implies that it is not possible to determine the phase of the Odderon mathematically

- This issue can be succinctly grasped: in the forward direction the physical amplitudes $\mathcal{F}^{pp}_{\bar{p}p}(s)$ can be written as $\mathcal{F}^{pp}_{\bar{p}p}(s) = F^{+}(s) \pm F^{-}(s)$

- Considering that the only relevant contributions are those arising from the Pomeron and the Odderon exchanges, we can write the symmetric and antisymmetric amplitudes as $F^{+}(s) = R_{\mathbb{P}}(s) + iI_{\mathbb{P}}(s)$ and $F^{-}(s) = R_{\mathbb{O}}(s) + iI_{\mathbb{O}}(s)$

From the optical theorem, we have $s\sigma_{tot}^{pp,\bar{p}p}(s) = 4\pi \,\mathrm{Im}\,\mathcal{F}_{\bar{p}p}^{pp}(s) > 0$, which implies that

$$\mathrm{Im}\,\mathcal{F}_{\bar{p}p}^{pp}(s) = I_{\mathbb{P}}(s) \pm I_{\mathbb{O}}(s) > 0$$

and, in turn,

$$I_{\mathbb{P}}(s) > |I_{\mathbb{O}}(s)|$$

As a consequence,

$$I_{\mathbb{P}}(s) = \frac{s}{2}\left[\sigma_{tot}^{pp}(s) + \sigma_{tot}^{\bar{p}p}(s)\right] > 0$$

while

$$I_{\mathbb{O}}(s) = \frac{s}{2}\left[\sigma_{tot}^{pp}(s) - \sigma_{tot}^{\bar{p}p}(s)\right]$$

is not bound by the same positivity requirements

Results

■ Since the absolute values of cross sections measured at the same energy by different groups do not agree, we have introduced normalization factors N_i for high-energy $d\sigma/dt$ data

$\Rightarrow$ $i = 7[A]$, $8[A]$, and $13[A]$ for the ATLAS/ALFA data and $i = 7[T]$, $8[T]$, and $13[T]$ for the TOTEM data (here the numbers within the indices i correspond to the values of $\sqrt{s}$)

$\Rightarrow$ Analogous normalization factors are introduced for the Tevatron data with $i = 1.8[E]$ and $i = 1.8[C]$, i.e. $N_{1.8[E]}$ for the E710 data and $N_{1.8[C]}$ for the CDF data

$\Rightarrow$ Despite being the only data set measured at $\sqrt{s} = 546$ GeV, we also included a normalization factor for $d\sigma^{\bar{p}p}/dt\big|_{\sqrt{s}=546\,\mathrm{GeV}}$, namely N_{546}

Results

- Furthermore, when dealing with the data sets incorporating normalization factors N_i, we make use of the formula

$$\chi^2 = \sum_{ij} \frac{(N_i ds_{ij}^{th} - ds_{ij}^{exp})^2}{(\delta_{ij}^{rem})^2} + \sum_i \frac{(1 - N_i)^2}{\delta_i^2}$$

$\Rightarrow$ i denotes the particular set of data while j denotes the point t_j in this set of data

$\Rightarrow$ ds^{th} is the theoretically calculated $d\sigma/dt$ cross section while ds^{exp} is the value measured at the same ij point experimentally

$\Rightarrow$ δ_i is the normalization uncertainty of the given (i) set of data and δ_{ij}^{rem} is the remaining error at the point ij calculated as $(\delta_{ij}^{rem})^2 = \delta_{tot,ij}^2 - \delta_i^2$

$\Rightarrow$ As a rule the value of δ^{rem} is dominantly the statistical error

Table: Values of the parameters obtained in the global fits to Ensemble $A \oplus T$.

	Model I	**Model II**	**Model II**
$\beta_{\mathbb{P}}(0)$	2.247±0.013	2.259±0.016	2.307±0.022
ϵ	0.1173±0.0021	0.1180±0.0020	0.1134±0.0019
$\alpha'_{\boldsymbol{P}}$ (GeV^{-2})	0.124±0.024	0.128±0.022	0.133±0.023
A (GeV^{-2})	5.01±0.20	4.78±0.21	4.72±0.21
B (GeV^{-4})	6.61±0.99	6.7±1.1	6.9±1.2
C (GeV^{-6})	20.4±5.7	17.7±4.0	17.0±4.2
$\beta_{\mathbb{O}}(0)$	(0.15 $\times 10^{-4}$) ±39	0.90±0.18	0.88±0.18
N_{546}	0.941	0.933	0.958
$N_{1.8[E]}$	0.923	0.912	0.944
$N_{1.8[C]}$	1.087	1.070	1.109
$N_{7[A]}$	1.015	1.015	1.056
$N_{8[A]}$	1.003	1.003	1.045
$N_{13[A]}$	1.009	1.009	1.052
$N_{7[T]}$	1.077	1.077	1.121
$N_{8[T]}$	1.121	1.121	1.167
$N_{13[T]}$	1.150	1.150	1.200
$\rho^{pp}(\sqrt{s} = 13$ TeV)	0.114	0.111	0.109
$\rho^{\bar{p}p}(\sqrt{s} = 13$ TeV)	0.114	0.119	0.116
Allowed N_i interval	[0.85,1.15]	[0.85,1.15]	[0.80,1.20]
ν	504	504	504
χ^2/ν	1.44	1.11	1.03